Journal of Pharmaceutical and Biomedical Analysis 53 (2010) 235–242

Contents lists available at ScienceDirect

Journal of Pharmaceutical and Biomedical Analysis

journal homepage: www.elsevier.com/locate/jpba

Synthesis and characterization of self-assembled CdHgTe/gelatin nanospheres as stable near infrared fluorescent probes in vivo

Yunqing Wang[a,b,c], Chao Ye[a,b], Liheng Wu[a,b], Yuzhu Hu[a,b,*]

[a] Key Laboratory of Drug Quality Control and Pharmacovigilance, Ministry of Education, Nanjing 210009, China
[b] Department of Analytical Chemistry, China Pharmaceutical University, Nanjing 210009, China
[c] Yantai Institute of Coastal Zone Research, Chinese Academy of Sciences, Yantai 264003, China

ARTICLE INFO

Article history:
Received 28 December 2009
Received in revised form 11 February 2010
Accepted 18 February 2010
Available online 25 February 2010

Keywords:
CdHgTe/gelatin nanospheres
Biomimetic synthesis
Fluorescent probes
Near infrared imaging
In vivo visible drug nanocarriers

ABSTRACT

This work presented a kind of novel near infrared emitting CdHgTe/gelatin nanospheres which were synthesized with $Cd(NO_3)_2$, $Hg(NO_3)_2$, NaHTe and a thiol stabilizer in gelatin solution. The self-assembled nanospheres were megranate-like and nearly 40 nm in diameter, with CdHgTe QDs uniformly embedded in gelatin matrix. They exhibited strong fluorescence ranging from 580 to 800 nm that could be tuned by molar ratios of Hg^{2+} and gelatin. The full widths at half-maximum of the emission spectra were in the range of 60–80 nm. Compared with bare CdHgTe QDs, the photostability of this compact complex nanostructure remarkably improved. Moreover, the fluorescence of CdHgTe/gelatin nanospheres was much more resistant to the interference from certain kinds of endogenous biomolecules such as HSA, transferrin and hemoglobin. Further applications of living cells and mouse imaging were demonstrated with an in vivo near infrared fluorescence imaging system. The inherent advantages of high stability as well as high fluorescence intensity make the nanospheres particular interested NIR bioprobe candidates for in vivo imaging studies.

1. Introduction

Near infrared (NIR) light (700–900 nm) possesses the capability of penetrating living tissues several centimeters due to the low absorbance of tissue intrinsic chromophores such as oxy- and deoxy-hemoglobin, melanin, water and lipid [1,2]. Based on this unique deeper tissue-penetrative property as well as non-ionizing and non-radioactive advantages, the research of NIR non-invasive imaging techniques attracted extensive attentions for real time and dynamic monitoring/tracing of biological signals in living animals. As a newly emerged optical technique, NIR imaging was successfully applied in many frontier fields of life sciences, such as nanomedicine research [3,4], cancer diagnosis and treatment [5,6] in recent years.

The selection of appropriate NIR fluorescent probes was very important for the successful application of NIR imaging technique. So far, there are quite few kinds of probes with NIR fluorescent emission. Most of them are organic dyes such as Cy7, IRDye78 and DIR that suffer from many inherent drawbacks of narrow excitation and wide emission spectra, ease to photobleach as well as high cost. NIR quantum dots (QDs) such as CdHgTe, CdTeSe/CdS are newly emerged inorganic fluorescent probes. They provide several advantages over organic fluorophores for biological imaging, including broad excitation spectra coupled with narrow, tunable emission spectra and high resistance to photobleaching [7]. Lately QDs have been severed as excellent alternatives of traditional dyes in many fluorescence based bioanalytical techniques [8–10]. Despite QDs possess many unique optical properties, quite a lot of problems are also noticed for in vivo biological imaging applications. For instance, due to the small size and large surface area, they tend to bind with biological molecules through non-specific adsorption or chemical reaction, which will result in agglomeration of QDs and subsequent fluorescence quenching, distorting the imaging signals. Besides, the heavy metal ions may release from QDs and induce potential biological toxicity. Hence, design and synthesis of novel NIR QDs probes that exhibit low non-specific interactions, high colloidal and optical stability as well as biocompatibility, is still a key issue for in vivo NIR imaging research.

Biomimetic synthesis is an attractive method for preparation of various inorganic nanocrystals. In this method, macromolecules with various functional groups and featured spatial structures are used as the synthesis templates. They are capable of controlling the nucleation and growth process of nanocrystals and also modulating the shape and physicochemical properties [11–13]. More importantly, the surface coating macromolecules passi-

* Corresponding author at: Key Laboratory of Drug Quality Control and Pharmacovigilance, Ministry of Education, Nanjing 210009, China. Tel.: +86 25 83271280; fax: +86 25 83271280.
E-mail address: njhuyuzu@126.com (Y. Hu).

0731-7085/$ – see front matter © 2010 Elsevier B.V. All rights reserved.
doi:10.1016/j.jpba.2010.02.028

vate the as-prepared nanocrystals and greatly improve their stability and biocompatibility. Gelatin is a kind of biocompatible polymer derived from collagen and is proved to be an ideal candidate of template for biomimetic synthesis of nanoparticles. Recently, it was reported as biological matrix for the in situ preparation of various novel nanomaterials with interesting morphology and excellent physicochemical property, such as Fe_3O_4 [14], FeCo [15] magnetic nanoparticles, Au nanoparticles [16] as well as CdSe [17] and CdTe [18] QDs. However, to the best of our knowledge, there is no report on the biomimetic synthesis of NIR CdHgTe QDs using gelatin as template until now.

In this work, we synthesized novel self-organized NIR fluorescence emitting CdHgTe/gelatin nanospheres with $Cd(NO_3)_2$, $Hg(NO_3)_2$, NaHTe and a thiol stabilizer in gelatin solution. Comparing with bare CdHgTe QDs, the obtaining compact polymer–QDs complex nanospheres exhibited remarkably improved fluorescence stability in many test conditions. Based on this virtue, they were further successfully applied for NIR imaging of living cells and mouse with the aid of an in vivo NIR fluorescence imaging system. The CdHgTe/gelatin nanospheres exhibited great potential as NIR fluorescent nanoprobes and traceable nanocarriers for real time drug research in living animals.

2. Experimental

2.1. Apparatus

The absorption spectra were acquired on a UV2100 UV-VIS spectrometer (Shimadzu, Japan). All fluorescence measurements were made with a Cary Eclipse spectrofluophotometer (Varian, USA) equipped with a 1 cm quartz cell. The transmission electron microscopy (TEM) images and energy dispersive spectrum (EDS spectrum) of CdHgTe/gelatin nanospheres were acquired on a Philips FEI Tecnai 20 G2 S-TWIN transmission electron microscope (Philips, Netherlands). Fluorescence image of labelled cells was visualized using an Olympus IX-51 fluorescent microscope and captured with a Retica digital camera. The pH measurements were made with a Model pHS-25 meter (Shanghai Leici Equipment Factory, China). The components of the NIR system was locally equipped as follows: for the fluorescence images, a NL-FC-2.0-763 laser (λ = 765.9 nm) light was coupled into NIR optical fiber bundle and defocused to provide a broad spot with even optical density shining on the surface of the mouse. A high sensitive NIR CCD camera (Princeton, America) was positioned 10 cm above the subjects. An 800 nm long pass filter (Chroma, Rockingham, VT) was put ahead of the CCD to block the excitation and ambient light, and thus to capture the emitted fluorescence from the tissue. The imaging taking was controlled by the matched software. Besides, another HLU32F400 808 nm laser (LIMO, Dortmund, Germany) is supplied as background light to obtain the profile of the subjected animal.

2.2. Reagents

$Cd(NO_3)_2{\cdot}4H_2O$, tellurium powder, $Hg(NO_3)_2{\cdot}1/2H_2O$ and $NaBH_4$ were purchased from Shanghai Reagent Company, mercaptoacetic acid (MPA) was acquired from Shanghai Lingfeng Reagent Company, gelatin (type A, average molecular weight 1.1×10^5 kDa) and rodamine B were purchased from Sinopharm Chemical Reagent Co., Ltd. Human serum albumin (HSA), transferrin and hemoglobin (both from bovine blood) were purchased from Sigma–Aldrich Chemical Co., Ltd. Bare CdHgTe QDs were locally synthesized according to our previous work [19]. All water used in the experiment was double distilled.

2.3. Synthesis of CdHgTe/gelatin nanospheres

NaHTe solution was prepared beforehand. Briefly, 40 mg of $NaBH_4$, 60 mg of tellurium powder and 3.0 mL of H_2O were added into a small flask in sequence and then the flask was put in a 40 °C water bath. The reacting system was stirred under the protection of N_2 and the black tellurium powder disappeared after 1 h, obtaining a clear purple NaHTe solution. 92.4 mg of $Cd(NO_3)_2{\cdot}4H_2O$ and 63 μL of MPA were added to 100 mL of H_2O, and the pH of the solution was adjusted to 11.2 with 1 M NaOH. Then different amount of $Hg(NO_3)_2$ solution (10 mg/mL) was added to the mixture. After the precipitate formed gradually dissolved by agitation, various volume of 5% gelatin solution was added, making its final concentration in the mixture as 0, 0.5, 1.0 and 2.0 mg mL^{-1}. The solution was stirred slowly for 2 h under nitrogen to facilitate a chelating balance. Then 500 μL of the as-prepared NaHTe solution was injected into the mixture quickly and the resulting solution was refluxed under open-air condition. The Cd^{2+}/NaHTe/MPA molar ratio was 1:0.5:2.4. CdHg(5%)Te, CdHg(10%)Te and CdHg(20%)Te denoted the samples prepared when the adding amount of Hg^{2+} was 5%, 10% and 20% mole ratio as calculated from the content of added Cd^{2+} in the precursor solution. Aliquots of reaction solutions were removed at regular intervals for UV–vis absorption and fluorescence characterization.

2.4. Characterization

The TEM equipped EDS spectroscopy was applied for morphology characterization and analysis of the elements composition and ratio. To prepare the TEM sample, a 5 μL droplet of nanosphere solution was dripped onto a carbon-coated copper grid and dried at room temperature.

The ultraviolet–visible absorption and fluorescence spectra of the samples obtained with various adding amount of gelatin, Hg^{2+} and reflux time were recorded. For photostability test, the working solution of 10^{-5} mol L^{-1} rhodamine B was prepared by accurately weighing 2.40 mg rhodamine B and dissolving into 500 mL water, and the as-prepared CdHgTe QDs and CdHg(10%)Te–gelatin 1.0 mg/mL-1 h nanospheres solutions were used without further treatment. The solutions were irradiated under a 20 W 254 nm UV lamp and the fluorescence intensities were recorded at 0, 2, 4, 6, 8 and 10 h intervals for photostability test. The pH dependent fluorescence features of bare QDs and CdHgTe/gelatin nanospheres were investigated. Both solutions were diluted 100 times with 0.05 mol L^{-1} phosphate buffer solutions adjusting to different pH before the signals scans. In order to study the influence of biomolecules, 20 μL CdHgTe QDs and CdHgTe/gelatin nanospheres solutions were diluted into 2.0 mL water in a quartz cell and fluorescence measurements were made after the addition of different amount of gelatin, HSA, transferrin and hemoglobin.

2.5. Living cells and mouse labelling

One hundred microliters of CdHg(10%)Te–gelatin 1.0 mg/mL-1 h nanosphere solution was added into the culture medium of human brain glioma cells in a 96-well plate. After incubation for 1 h the cells were washed with phosphate buffer and observed under a fluorescence microscope immediately. A mouse was denuded by a mixture of Na_2S (5%) and starch followed immediately by daubing camphor ice to avoid further skin erosion. After resting for 24 h, the mouse was anesthetized with an intraperitoneal injection of 150 μL ethyl carbamate (20 mg/mL) and then immobilized in a lucite jig. Twenty hundred microliters of the as-prepared CdHg(20%)Te–gelatin1.0 mg/mL-1 h nanospheres solution was injected through the tail vein into the mouse. The NIR excitation light intensity of laser from the fiber bundle was

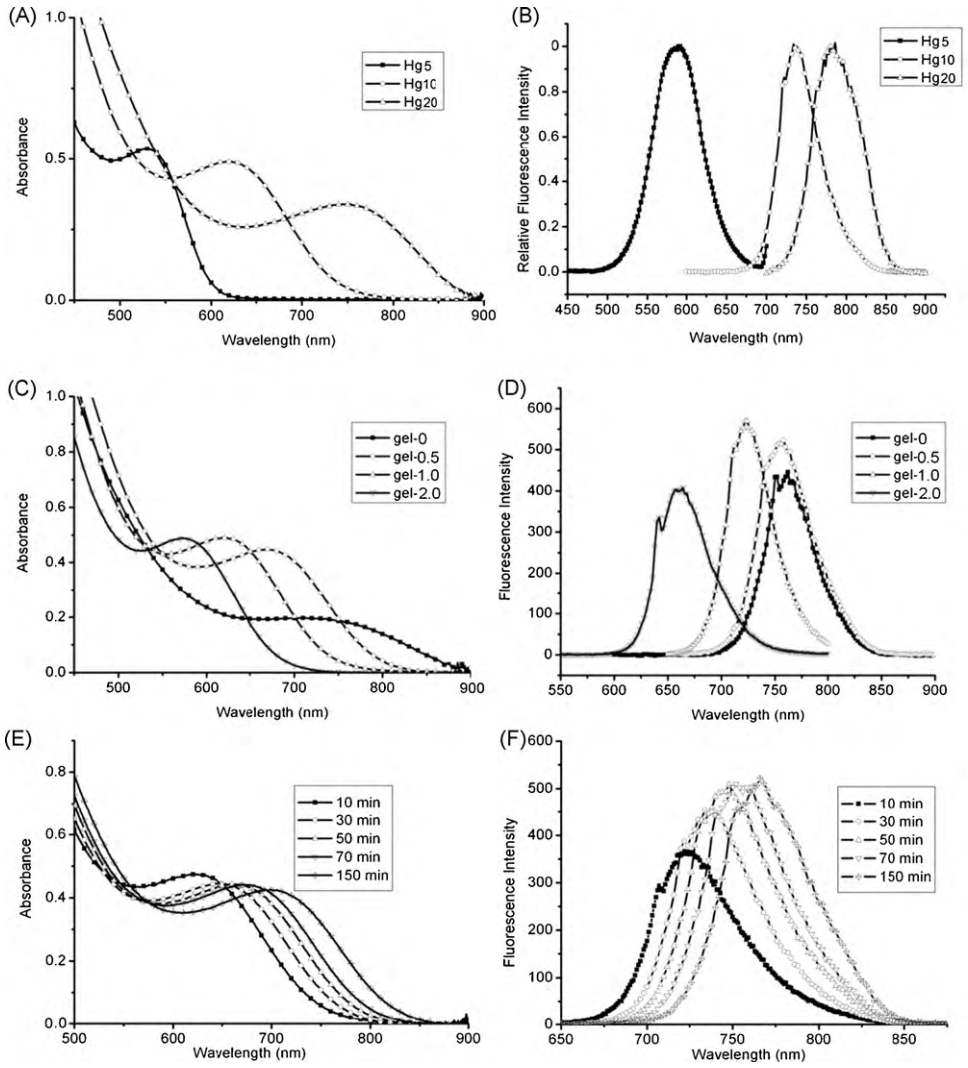

Fig. 1. Absorption and fluorescence spectra of CdHgTe/gelatin nanospheres with various amount of Hg^{2+} (A and B), gelatin (C and D) and different refluxing time (E and F). In (A) and (B), the adding amount of Hg^{2+} was 5%, 10% and 20% mole ratio as calculated from the content of added Cd^{2+} in the precursor solution. In (C) and (D), the concentration of gelatin was 0, 0.5, 1.0 and 2.0 mg mL^{-1}.

adjusted at 26 mW, which kept the same during the experiment. A series of images were then collected at 10 s, 5 min, 10 min and 2 h post-injection.

3. Results and discussion

3.1. The influence of synthesis conditions on spectroscopic properties

CdHgTe/gelatin nanospheres of different compositions were synthesized by controlling the adding amount of the Hg^{2+} and gelatin. The effect of Hg^{2+} on the optical properties of the nanospheres was firstly investigated. The concentration of gelatin of the reaction system was fixed at 1.0 mg mL^{-1}, while the adding amount of $Hg(NO_3)_2$ was made as 5%, 10% and 20% of the mole content of $Cd(NO_3)_2$ in the precursor. The absorption and fluorescence spectra of the samples refluxed for 1 h was shown in Fig. 1(A) and (B). It was apparent that with the increasing content of Hg^{2+}, the absorption spectra moved to a longer wavelength range accompanied by the expansion of the spectra bands. The fluorescence emission peaks were located at 586 nm, 740 nm and 775 nm, respectively, which also showed a red-shift discipline. These results indicated that the optical properties of the fluorescent nanoparticles were dependent on their chemical composition to a large extent, which was in consistent with the results of the CdHgTe QDs synthesis in pure aqueous medium [20].

The content of gelatin in reaction mixture also played an important role in modulating the absorption and emission peak position of the nanospheres. As could be seen in Fig. 1(C) and (D), when fixed the adding amount of Hg^{2+} for 10% and the refluxing time for 1 h, the increasing amount of gelatin led to blue shift of both spectra.

As is well known, the reaction time is another key parameter for the synthesis of QDs. When the contents of Hg^{2+} and gelatin was 10% and 0.5 mg mL^{-1}, respectively, with the increasing reaction time, the maximum absorption wavelengths red-shifted from 624 nm at 10 min to 695 nm at 150 min, and fluorescence peaks moved from 725 nm to 772 nm. Meanwhile, it could also be noticed that the half peak widths increased from 52 nm to 66 nm, indicating the broadening of QDs size distribution (Fig. 1(E) and (F)).

3.2. TEM and EDS characterization

Fig. 2(A) shows a typical TEM image of the CdHgTe/gelatin nanospheres. It was showed that the nanospheres were uniform with an average size around 40 nm. An image with higher mag-

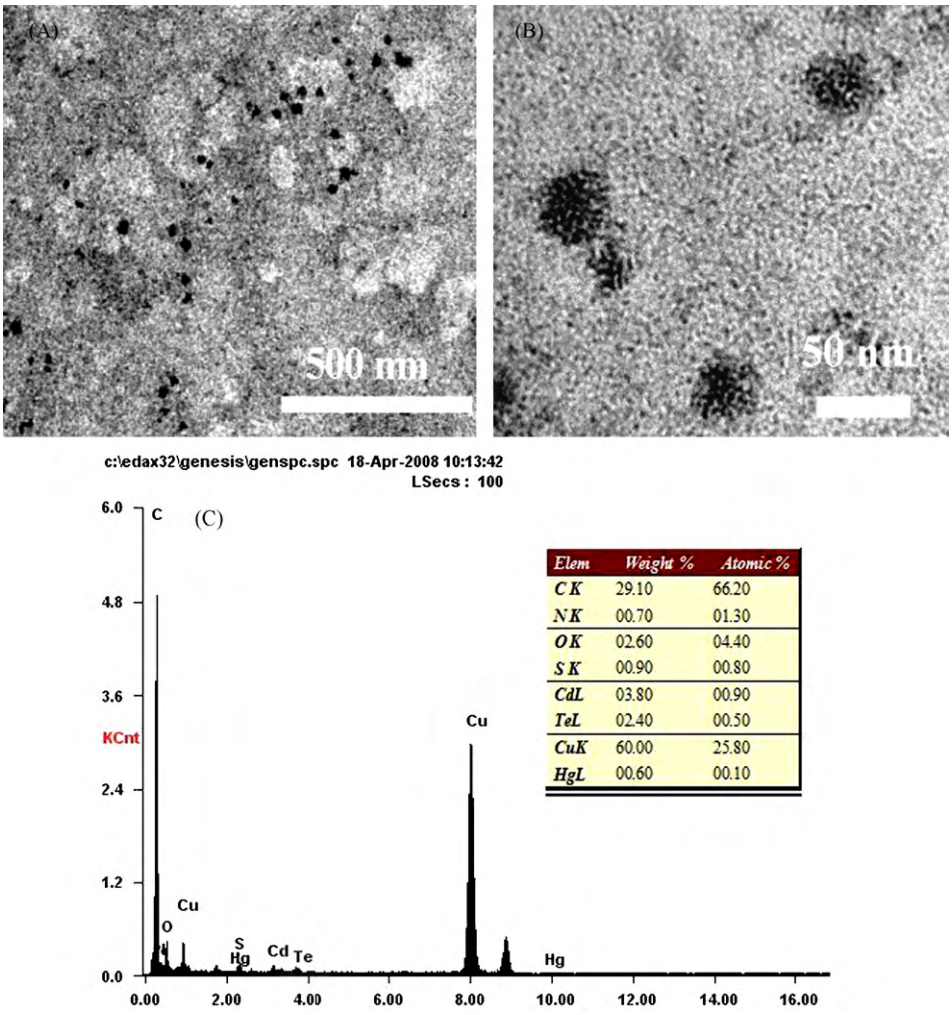

Fig. 2. TEM images (A and B) and EDS spectrum (C) of CdHgTe/gelatin nanospheres.

nification (Fig. 2(B)) revealed that primary small CdHgTe QDs were well assembled into the interior of nanospheres, forming a megranate-like complex structure. Fig. 2(C) shows the EDS spectra and elemental analysis table of the complex specimen. It was obvious that the strong signals of copper, carbon and oxygen elements were attributed to the copper grid and carbon supporting membrane. The signals of cadmium, mercury and telluride elements were originated from the CdHgTe QDs embedded in the nanospheres and the signal of sulfur was from the capping ligands of MPA. While the nitrogen component of nanospheres, which was not detectable for bare CdHgTe QDs, clearly proved the existence of gelatin polypeptide chains.

3.3. Formation mechanism

By integrating the information of TEM, EDS elemental analysis and spectroscopic properties of different synthesis conditions, we further proposed a formation mechanism of CdHgTe/gelatin nanospheres (Fig. 3). In aqueous solution gelatin molecule showed a random coil structure with a hydrodynamic diameter around 40 nm [21]. When the metal ion precursors of Hg-MPA and Cd-MPA were added into gelatin matrix, they were bond and in situ immobilized to abundant amino and carboxylic groups of gelatin through electrostatic and hydrogen bond interaction. After adding NaHTe, the original crystal formation process of CdHgTe QDs occurred in these separate binding sites of single gelatin molecule. With the growth of QDs, the self-assembly, single gelatin molecule-template nanospheres with various CdHgTe QDs encapsulated formed consequently.

Due to the synergistic multidentate coordination by random gelatin chains as well as high viscosity of the reaction matrix, the diffusion of the ion precursors throughout the system was hindered, which greatly decreased the growth rate of nanocrystals. As a consequence, the Ostwald ripening process of QDs occurred at a

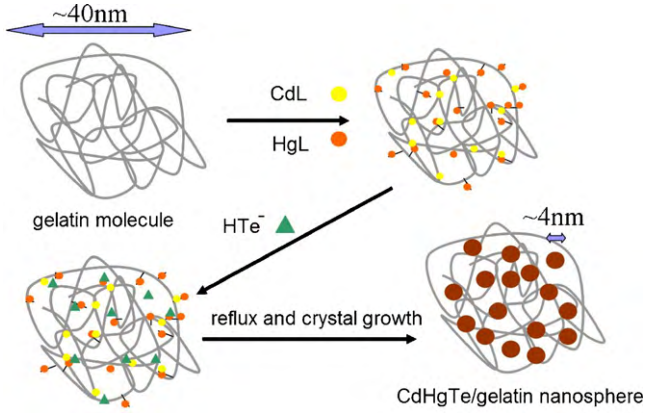

Fig. 3. Schematic illustration of the formation mechanism of CdHgTe/gelatin nanospheres.

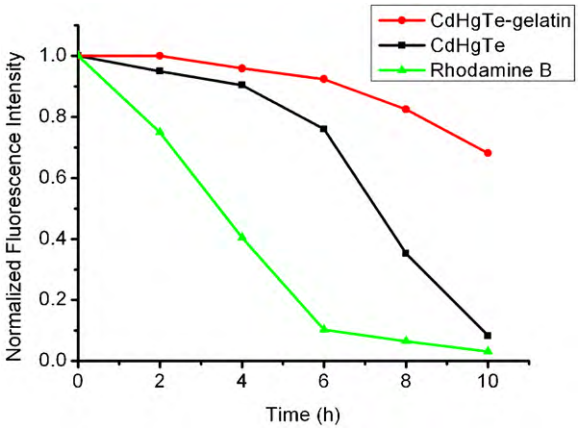

Fig. 4. Comparison of anti-quenching ability of rhodamine B, CdHgTe QDs and CdHgTe/gelatin nanospheres. The as-prepared CdHgTe QDs and CdHgTe/gelatin nanospheres solutions were selected without dilution. The concentration of rhodamine B was 10^{-5} mol L^{-1}.

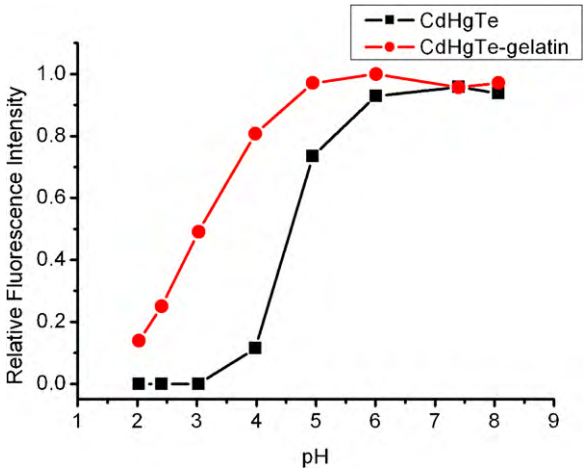

Fig. 5. The influence of pH on the fluorescence of CdHgTe QDs and CdHgTe/gelatin nanospheres. The pH of buffer was 2.03, 2.41, 3.03, 3.98, 4.95, 6.01, 7.40 and 8.07, respectively.

slower rate initially as the nucleation centers took longer to interact. Hence, comparing with pure aqueous system, gelatin matrix enabled the QDs to grow more discretely and gave rise to spectroscopic properties blue shift. On the other hand, with the increasing amount of gelatin in the reaction system, mercury ions were well dispersed and bond to more initial nucleation sites, and therefore decreasing the mercury content of QDs synthesized in situ. This finally resulted in the blue shift of both absorption and fluorescence spectra.

3.4. Photostability investigation

As shown in Fig. 4, under the irradiation of UV light, the fluorescence of rodamine B decreased sharply, and completely vanished after 10 h. In an unsealed system, the fluorescence of CdHgTe QDs was more stable in the first 4 h, which showed a decrease of 8% of its original intensity. However, with prolonged irradiation time, it could be clearly observed that QDs were severely oxidized, which resulted in turbidity of the solution with suspended silvery white sediment. This oxidation process could greatly accelerate the decrease rate of fluorescence intensity, making it also disappeared in 10 h as a result. By contrast, the anti-photobleaching ability of CdHgTe/gelatin nanospheres was superior to both of the former counterparts. After irradiation for 10 h, the solution was still clear and 76% of the original fluorescence was retained. These results illustrated that the surface coating gelatin of the nanospheres could effectively prevent CdHgTe QDs from oxidation, which was benefit for the increase of their photostability.

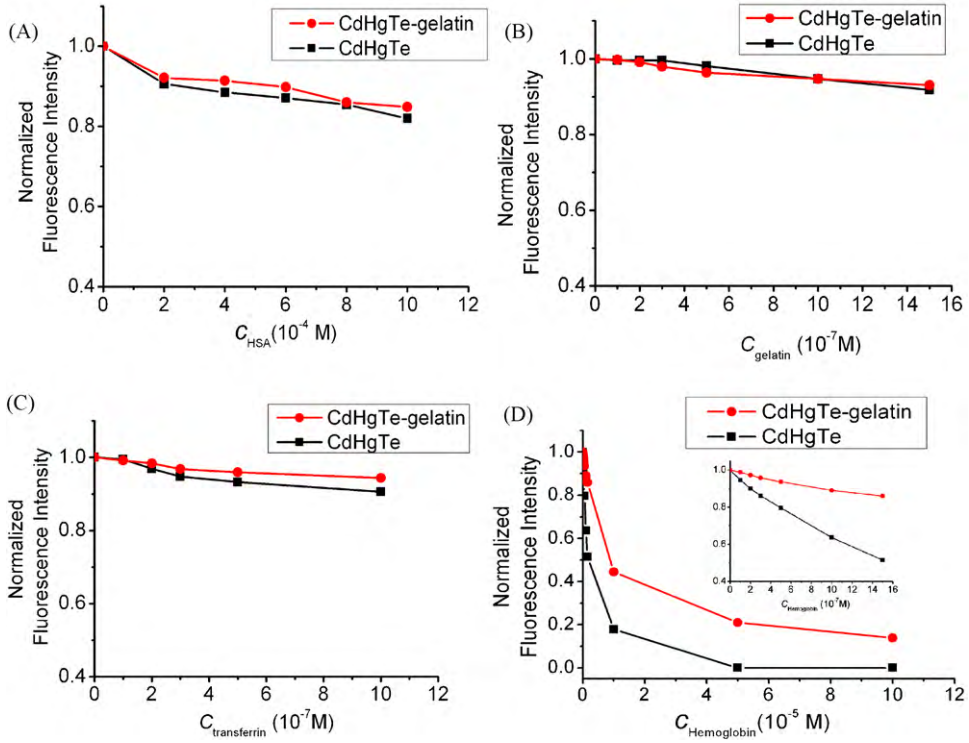

Fig. 6. The influence of various proteins on the fluorescence intensity of CdHgTe QDs and CdHgTe/gelatin nanospheres. The concentrations of gelatin, HSA and hemoglobin were 0, 1, 2, 3, 5, 10 and 15×10^{-7} mol L^{-1}. The concentration of transferrin was 0, 1, 2, 3, 5 and 10×10^{-7} mol L^{-1}.

3.5. The influence of pH on the fluorescence intensity of nanospheres

The fluorescence of CdHgTe QDs was very sensitive to pH in the acidic environment. With pH decrease, the fluorescence intensity decreased sharply. As can be seen in Fig. 5, the fluorescence intensity at pH 4 was only 10% of the maximum value at neutral condition, while the fluorescence was completely quenched when the pH dropped to 3. Compared with bare QDs, the effect of pH on the fluorescence of nanospheres was weakened remarkably. When the pH of the nanosphere solution was 4, the fluorescence intensity was still kept 82% of the maximum value, and apparent signal could also be detected at pH as low as 2. Previous studies showed that metal ion–MPA complexes bond on the surface of QDs contributed to the fluorescence enhancement and stability of QDs. The increasing of H^+ would cause the decomposition of the annulus of the metal ion–MPA complexes due to the protonation of the surface-binding thiolates. Besides, the protonation process of carboxylate groups from particle surface-binding MPA became strong, which also led to the fluorescence quenching of MPA-stabilized QDs [22]. For nanospheres, the amphoteric gelatin macromolecules could accept H^+ and be positive charged, severing as "pH buffers" around the embedded QDs. This would protect the surface of QDs from direct contact with H^+ and therefore enhanced the stability in acidic atmosphere.

3.6. The influence of proteins on the fluorescence intensity of nanospheres

It is important for in vivo NIR fluorescence probes to resist the non-specific adsorption in complex biological system. In order to investigate the influence of the inherent biomolecules on the fluorescence intensity of both bare QDs and gelatin nanospheres, four kinds of proteins were chosen in the test. Because albumin in serum is several $g\,L^{-1}$, which corresponds to sub $mmol\,L^{-1}$, a high concentration range of 0.1–1.0 mmol was used in the study. As shown in Fig. 6, gelatin and HSA molecules did not result in obvious variations of fluorescence intensity for both CdHgTe QDs and the nanospheres. However, the addition of transferrin and hemoglobin induced remarkable quenching of bare CdHgTe QDs, while the fluorescence intensity of the complex nanospheres was relatively stable. The quenching of QDs by transferrin and hemoglobin could be explained as follows: when QDs and proteins mixed, compact QDs–protein complex firstly formed due to the electrostatic adsorption. Under photo-irradiation the electrons within the CdHgTe QDs were excited to the excited state. Both Fe(III) containing proteins (denoted as [Fe(III)-trans/hemo], trans and hemo were for transferring and hemoglobin, respectively) could directly intercept one of the charge carriers and was reduced to [Fe(II)-trans/hemo] for the proximity between QDs and proteins. This process could disrupt the radiative recombination of the holes and the excited electrons and quench the fluorescence of the CdHgTe QDs [23]. For the complex nanospheres, the encapsulated QDs could hardly get enough proximity to these interference proteins and achieve the electron transfer process because of the protection of gelatin, thus greatly weakened the quenching effect. Interestingly, when CdHgTe QDs and QDs–gelatin nanospheres were added in the whole blood of mouse in vitro, they can both emit bright fluorescence. This may because hemoglobin in blood was almost all contained in red blood cells, and the free hemoglobin in serum that can directly affect the property of QDs was scarce.

3.7. Biological NIR fluorescence imaging for living cells and mouse

The fluorescence images of human brain glioma cells after incubating with CdHgTe/gelatin nanospheres were shown in Fig. 7. Red fluorescence was observed in the cells, which suggested that the nanospheres were small enough to be taken up by the cells, and the fluorescence of QDs was not quenched in the interior of cells. Moreover, no morphological change of the cells was observed during the incubation period of 24 h, which indicated that the nanospheres were biocompatible.

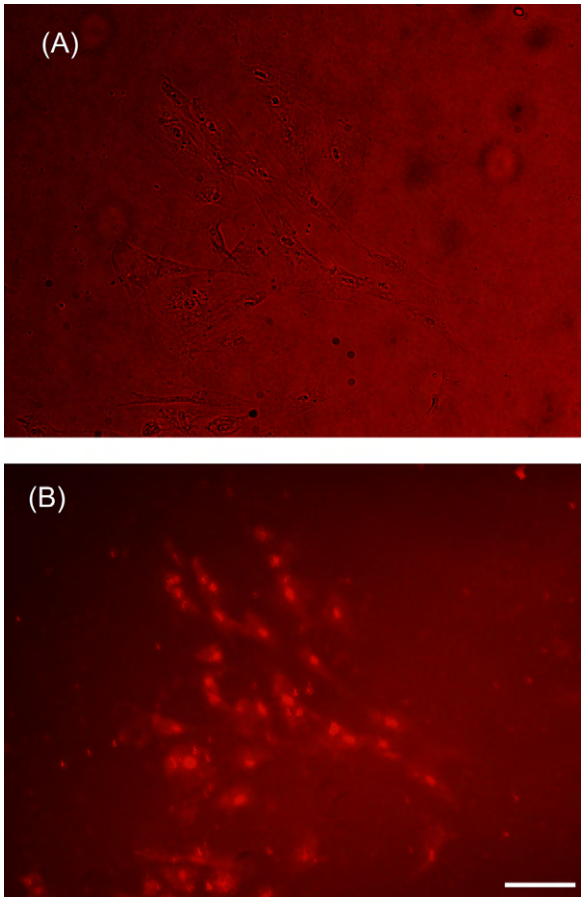

Fig. 7. The bright field (A) and fluorescence (B) images of CdHgTe/gelatin nanospheres labeling human brain glioma cells. The scale bar was 10 μm.

Fig. 8 represents a series of in vivo images taken by the NIR imaging system at different time interval after CdHgTe/gelatin nanospheres injection. After 200 μL of CdHgTe/gelatin nanophore solution was injected through the tail vein, fluorescence images of the mouse was acquired at 10 s, 5, 10 and 120 min. Photos indicated that the nanospheres immediately distributed to all over the vessels by blood circulation after tail vein injection. A network of blood vessels could be distinguished in the fluorescence images and the dynamic changes of nanospheres in the superficial vessels were clearly observed. With the distribution of the fluorescent nanospheres in the blood circulation system, some of the deeper vessels also presented in the network, which made the whole body exhibit strong fluorescence signal, as can be seen in Fig. 8(B). And then CdHgTe/gelatin nanospheres were observed to arrive at liver tissue within 10 min, and the signal from the body decreased sharply. The fluorescence signals disappeared in the mouse body and could be merely observed in liver 2 h after injection.

This in vivo behaviour of was quite different from that of bare QDs reported in previous work [19]. For CdHgTe QDs, besides accumulating in liver, a portion of them were observed to enter other organs such as intestine an hour after injection and cleared within several hours. We suppose that the different particle size

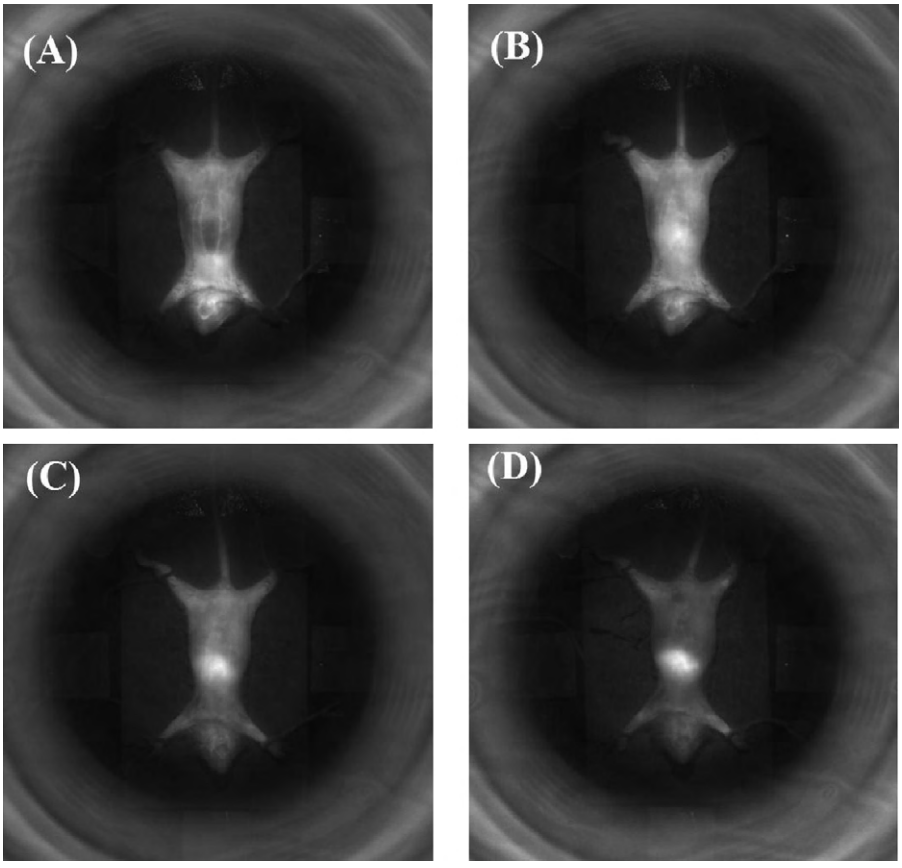

Fig. 8. NIR images of the mouse after CdHgTe/gelatin nanospheres solution was injected via tail vein. (A–D) Fluorescence image of the same mouse after injection for 10 s, 5, 10 and 120 min, respectively.

might be a key reason that made a distinction of their distribution behaviour, because the bigger QDs–gelatin nanospheres are easier to be detected and phagocytized by defensive system such as Kupffer cells in liver. Similar findings were also reported in the study of CdTe QDs [24] and gold nanoparticles [25]. Since QDs–gelatin nanospheres could quickly accumulate in liver after intravenous injection, they might be useful for diagnosis and treatment of liver disease such as hepatoma and cirrhosis.

4. Conclusion

We reported on biomimetic synthesis of novel NIR emitting CdHgTe/gelatin nanospheres with gelatin molecules as templates. The self-organized nanospheres remarkably improved the photostability and were qualified for imaging of living cells and mouse, illustrating great potential for NIR bio-imaging. Owing to numerous surface active sites provided by gelatin, the CdHgTe/gelatin nanospheres have advantage over QDs for further functionalized modification, which is helpful for the design and synthesis of cancer targeting and diagnosis probes. Besides, the nanospheres with huge accessible surface area can also acted as promising traceable nanocarriers for proteins, DNA and small molecules in the research of in situ, real time monitoring of drug release and therapy studies in the future.

Acknowledgment

We wish to acknowledge the financial support of the National Natural Science Foundation of China (Grant No. 30873197).

References

[1] B. Riefke, K. Licha, W. Semmler, Contrast agents for optical mammography, Radiologe 37 (1997) 749–755.
[2] N. Hanaoka, Y. Aoyama, M. Kameyama, M. Fukuda, M. Mikuni, Deactivation and activation of left frontal lobe during and after low-frequency repetitive transcranial magnetic stimulation over right prefrontal cortex: a near-infrared spectroscopy study, Neurosci. Lett. 414 (2007) 99–104.
[3] J. Zhang, H.Y. Chen, L. Xu, Y.Q. Gu, J. Control. Release 131 (2008) 34–40.
[4] P.P. Ghoroghchian, P.R. Frail, K. Susumu, D. Blessington, A.K. Brannan, F.S. Bates, B. Chance, D.A. Hammer, M.J. Therien, Proc. Natl. Acad. Sci. U.S.A. 102 (2005) 2922–2927.
[5] V. Kalchenko, S. Shivtiel, V. Malina, K. Lapid, S. Haramati, T. Lapidot, A. Brill, A. Harmelina, Use of lipophilic near-infrared dye in whole-body optical imaging of hematopoietic cell homing, J. Biomed. Opt. 11 (2006), 050507.
[6] D. Granot, Y. Addadi, V. Kalchenko, A. Harmelin, L.A. Kunz-Schughart, M. Neeman, In vivo imaging of the systemic recruitment of fibroblasts to the angiogenic rim of ovarian carcinoma tumors, Cancer Res. 67 (2007) 9180–9189.
[7] S. Kim, Y.T. Lim, E.G. Soltesz, J. Lee, A. Nakayama, J.A. Parker, T. Mihaljevic, R.G. Laurence, D.M. Dor, L.H. Cohn, M.G. Bawendi, J.V. Frangioni, Near-infrared fluorescent typeIIquantum dots for sentinel lymph node mapping, Nat. Biotechnol. 22 (2004) 93–97.
[8] N.Y. Morgan, S. English, W. Chen, V. Chernomordik, A. Russo, P.D. Smith, A. Gandjbakhche, Real time in vivo non-invasive optical imaging using near-infrared fluorescent quantum dots, Acad Radiol. 12 (2005) 313–323.
[9] W. Cai, D. Shin, K. Chen, O. Gheysens, Q. Cao, S. Wang, S.S. Gambhir, X. Chen, Peptide-labeled near-infrared quantum dots for imaging tumor vasculature in living subjects, Nano Lett. 6 (2006) 669–676.
[10] Y. Guo, D. Shi, H. Cho, Z. Dong, A. Kulkarni, G.M. Pauletti, W. Wang, J. Lian, W. Liu, L. Ren, Q. Zhang, G. Liu, C. Huth, L. Wang, R.C. Ewing, In vivo imaging and drug storage by quantum-dot-conjugated carbon nanotubes, Adv. Funct. Mater. 18 (2008) 2489–2497.
[11] X. Fu, Y. Wang, L. Huang, Y. Sha, L. Gui, L. Lai, Y. Tang, Assemblies of metal nanoparticles and self-assembled peptide fibrils-formation of double helical and single-chain arrays of metal nanoparticles, Adv. Mater. 15 (2003) 902–906.
[12] D. Qin, X. Ma, L. Yang, L. Zhang, Z. Ma, J. Zhang, Biomimetic synthesis of HgS nanoparticles in the bovine serum albumin solution, J. Nanopart. Res. 10 (2008) 559–566.

[13] X. Zhang, J. Chen, P. Yang, W. Yang, Biomimetic synthesis silver crystallite by peptide AYSSGAPPMPPF immobilized on PET film in vitro, J. Inorg. Biochem. 99 (2005) 169–1697.
[14] B. Gaihre, S. Aryal, N.A.M. Barakat, H.Y. Kim, Gelatin stabilized iron oxide nanoparticles as a three dimensional template for the hydroxyapatite crystal nucleation and growth, Mater. Sci. Eng. C: Biol. 28 (2008) 1297–1303.
[15] L. Dong, S. Liu, H. Gao, N. Ding, W. Tremel, C. Xiong, Q. Zhu, W. Knoll, Self-assembled FeCo/gelatin nanospheres with rapid magnetic response and high biomolecule-loading capacity, Small 5 (2009) 1153–1157.
[16] L. Lu, K. Ai, Y. Ozaki, Environmentally friendly synthesis of highly monodisperse biocompatible gold nanoparticles with urchin-like shape, Langmuir 24 (2008) 1058–1063.
[17] A.E. Raevskaya, A.L. Stroyuk, S.Y. Kuchmiy, Y.M. Azhniuk, V.M. Dzhagan, V.O. Yukhymchuk, M.Y. Valakh, Growth and spectroscopic characterization of CdSe nanoparticles synthesized from $CdCl_2$ and Na_2SeSO_3 in aqueous gelatin solutions, Colloid Surf. A 290 (2006) 304–309.
[18] S.J. Byrne, Y. Williams, A. Davies, S.A. Corr, A. Rakovich, Y.K. Gunko, Y.P. Rakovich, J.F. Donegan, Y. Volkov, Synthesis and cytotoxicity studies of CdTe quantum dot-gelatin nanocomposites, Small 3 (2007) 1152–1156.
[19] H. Chen, Y. Wang, J. Xu, J. Ji, J. Zhang, Y. Hu, Y. Gu, Non-invasive near infrared fluorescence imaging of CdHgTe quantum dots in mouse model, J. Fluores. 18 (2008) 801–811.
[20] H. Qian, C. Dong, J. Peng, X. Qiu, Y. Xu, J. Ren, High-quality and water-soluble near-infrared photoluminescent CdHgTe/CdS quantum dots prepared by adjusting size and composition, J. Phys. Chem. C 111 (2007) 16852–16857.
[21] A. Saxena, T. Antony, H.B. Bohidar, Dynamic light scattering study of gelatin-surfactant interactions, J. Phys. Chem. B 102 (1998) 5063–5068.
[22] M.Y. Gao, S. Kirstein, H. Möhwald, Strongly fluorescent CdTe nanocrystals by proper surface modification, J. Phys. Chem. B 102 (1998) 8360–8363.
[23] D. Hu, H. Wu, J. Liang, H. Han, Study on the interaction between CdSe quantum dots and haemoglobin, Spectrochim. Acta A 69 (2007) 830–834.
[24] H.C. Fischer, L. Liu, K.S. Pang, W.C.W. Chan, Pharmacokinetics of nanoscale quantum dots: in vivo distribution, sequestration, and clearance in the rat, Adv. Funct. Mater. 16 (2006) 1299–1305.
[25] G. Terentyuk, G. Akchurin, I. Maksimova, A. Shantrokha, V. Tuchin, G. Maslyakova, L. Suleymanova, B. Kogan, N. Khlebtsov, B. Khlebtsov, Tracking gold nanoparticles in the body, SPIE Newsroom (2009) doi:10.1117/2.1200907.1619.